Laboratory Investigation (2020) 100:363–377
https://doi.org/10.1038/s41374-019-0316-8

ARTICLE

The Shh/Gli signaling cascade regulates myofibroblastic activation of lung-resident mesenchymal stem cells via the modulation of Wnt10a expression during pulmonary fibrogenesis

Honghui Cao[1,2] · Xiang Chen[1,2] · Jiwei Hou[1,2] · Cong Wang[3] · Zou Xiang[4] · Yi Shen[5] · Xiaodong Han[1,2]

Received: 14 January 2019 / Revised: 16 August 2019 / Accepted: 16 August 2019 / Published online: 20 September 2019

Abstract

Lung-resident mesenchymal stem cells (LR-MSCs) are important regulators of lung repair and regeneration, and evidence suggests that this cell population also plays a vital role in fibrosis. Crosstalk between sonic hedgehog (Shh) signaling and wingless/integrated (Wnt) has been demonstrated in idiopathic pulmonary fibrosis (IPF). However, the underlying correlation between LR-MSCs and the Shh-Wnt signaling cascade remains poorly understood. Here, we identified Wnt10a as a key factor in pulmonary fibrosis. Using a bleomycin mouse model, we found that highly expressed Wnt10a was secreted by LR-MSCs undergoing myofibroblastic differentiation. LR-MSCs with myofibroblast characteristics isolated from fibrotic lungs exhibited increased Shh pathway activity, suggesting their role as Shh targets. In vitro, LR-MSCs responded to stimulation by recombinant Shh, acquiring a myofibroblast phenotype. We further demonstrated that the Shh/glioblastoma (Gli) system machinery regulated LR-MSC-to-myofibroblast transition and pulmonary fibrosis via manipulation of Wnt/β-catenin signaling. Accordingly, inhibition of the Shh-Wnt signaling cascade prevented LR-MSC transformation into myofibroblasts and ameliorated pulmonary fibrotic lesions. Moreover, induction of Wnt10a expression and activation of Shh/Gli signaling were confirmed in human pulmonary fibrosis. In summary, this study linking the Shh-Wnt signaling cascade with LR-MSC fibrogenic activity furthered the current understanding of pulmonary fibrosis pathogenesis and might provide a new perspective in the development of treatment strategies for IPF.

Supplementary information The online version of this article (https://doi.org/10.1038/s41374-019-0316-8) contains supplementary material, which is available to authorized users.

✉ Yi Shen
yishen305@126.com

✉ Xiaodong Han
hanxd@nju.edu.cn

1 Immunology and Reproduction Biology Laboratory & State Key Laboratory of Analytical Chemistry for Life Science, Medical School, Nanjing University, 210093 Nanjing, China

2 Jiangsu Key Laboratory of Molecular Medicine, Nanjing University, 210093 Nanjing, China

3 State Key Laboratory of Natural Medicines and Jiangsu Key Laboratory of Drug Discovery for Metabolic Diseases, Center of New Drug Discovery, China Pharmaceutical University, 24 Tong Jia Xiang, 210009 Nanjing, China

4 Department of Health Technology and Informatics, Faculty of Health and Social Sciences, The Hong Kong Polytechnic University, Hung Hom, Kowloon, Hong Kong, China

5 Department of Cardiothoracic Surgery, Jinling Hospital, Medical School of Nanjing University, Nanjing, China

Introduction

Idiopathic pulmonary fibrosis (IPF) is a lethal lung disease defined as a specific form of chronic, irreversible interstitial pneumonia with poor prognosis. The annual incidence of IPF, occurring primarily in older adults, is estimated to be between 4.6 and 16.3 per 100,000 people [1–3]. Despite the increasing prevalence of this devastating disease, current clinical treatment options are limited and often undesirable. Thus, delineating the pathogenic mechanism underlying IPF is essential for the development of effective therapeutic strategies.

Emerging evidence suggests that activated mesenchymal cells contribute to the formation of fibroblastic foci and accumulation of extracellular matrix (ECM), leading to the distortion of lung structures [4]. Mesenchymal stem cells (MSCs) are adult connective tissue progenitor cells with multilineage differentiation potential that can be induced to differentiate into various cell types [5]. Tissue MSCs are generally believed to exist in most mammalian organs, including the lung, and to play a significant role in

the development of fibrotic diseases [6, 7]. Indeed, MSCs have been found to reside in interstitial perivascular niches throughout the alveolar-capillary network in the lungs of both mice and humans. These lung-resident mesenchymal stem cells (LR-MSCs) possess typical characteristics shared by other tissue-specific MSCs, including self-renewal ability, multipotent differentiation capacity, and autocrine or paracrine properties [8–10]. Importantly, the behavior of LR-MSCs is highly sensitive to the microenvironment to which they are exposed. These cells can be driven by local profibrotic factors to undergo a myofibroblastic transition that participates in the development of pulmonary fibrosis [11].

We previously found that canonical wingless/integrated (Wnt) signaling is activated in the lungs of bleomycin-treated mice and regulates myofibroblastic differentiation of LR-MSCs [12, 13]. This profibrotic pathway is mediated by Wnt proteins, a family of 19 secreted glycoproteins. When Wnt binds to the frizzled (Fzd) receptor along with low-density lipoprotein receptor-related protein (LRP), β-catenin is phosphorylated at Ser675 and subsequently translocates into the nucleus, where it activates T-cell factor/lymphoid enhancer binding factor (TCF/LEF) to promote the transcription of target genes [14, 15]. Recent studies demonstrated that the expression levels of Wnt family members were low in normal lungs but markedly elevated in the lungs of IPF patients [16, 17]. Therefore, these Wnts with altered expression may act as critical factors in the development of pulmonary fibrosis.

The sonic hedgehog (Shh) signaling is reported to regulate the expression of Wnt molecules by recruiting the transcription factor glioblastoma (Gli) to the promoters of Wnt genes [18, 19]. Similar to activation of the Wnt/β-catenin pathway, activation of Shh signaling in IPF has been documented in multiple studies [20–22]. Shh signaling maintains lung homeostasis or participates in lung disorders by regulating the differentiation of various types of hedgehog (Hh)-responsive progenitor or stem cells [22, 23]. Shh, the most widely studied and the most well-characterized Hh pathway ligand, is a soluble, lipid-modified morphogen [24]. As a secreted extracellular signal protein, Shh binds with the Patched (Ptc) receptor on the surface of Hh-responsive cells. This ligand-receptor interaction prevents Ptc from sequestering its coreceptor Smoothened (Smo), thereby freeing Smo to signal to the Gli. Activated Gli then translocates to the nucleus and promotes the transcription of downstream target genes, including several components of Shh signaling, such as Ptc, Gli1, and Gli2. In the absence of ligands, Ptc interacts with and suppresses Smo, resulting in inhibition of the Hh pathway [25, 26]. The factor Hh-interacting protein (Hhip) can also block Hh signaling via binding with Hh ligands to abrogate the Hh ligand-Ptc receptor interaction [27]. Despite a clear, important role of the Shh pathway in IPF, the mechanisms by which it affects the differentiation of LR-MSCs in pulmonary fibrogenesis remains elusive.

In this study, we discovered that bleomycin exposure induced Wnt10a expression in LR-MSCs undergoing myofibroblastic differentiation, a fibrotic event regulated by the Shh/Gli signaling cascade. Blockade of the Shh pathway or inhibition of Wnt proteins prevented LR-MSC-to-myofibroblast transition and alleviated pulmonary fibrosis. Furthermore, we confirmed Wnt10a upregulation and Shh/Gli signaling activation in human pulmonary fibrosis, suggesting that a similar mechanism is involved in IPF progression.

Materials and methods

Main reagents

Osteogenesis and adipogenesis differentiation kits were purchased from Invitrogen (Carlsbad, CA, USA). Alizarin red stain and oil red O solution were obtained from Millipore (Billerica, MA, USA). Bleomycin was purchased from Nippon Kayaku (Tokyo, Japan). Recombinant mouse Shh was purchased from eBioscience (San Diego, CA, USA). The Gli inhibitor Gant61 and Wnt/Fzd/LRP complex inhibitor salinomycin were obtained from Selleckchem (Houston, TX, USA). The antibodies used in this study are listed in Supplementary Table 1.

Cell culture and transfection

Primary mouse and human LR-MSCs were isolated as previously reported [9, 28, 29]. Freshly isolated cells were cultured at concentrations higher than 10^5 cells/ml in DMEM containing 10% fetal bovine serum, 4% L-glutamine, 1% nonessential amino acids and 1% penicillin and streptomycin and were maintained in a humidified atmosphere of 95% air and 5% CO_2 at 37 °C. Cells were passaged at 70–90% confluence in a 1:2 ratio using 0.25% trypsin. LV-Wnt10a-siRNA was synthesized by GENECHEM (Shanghai, China). Viral transfection was performed according to the manufacturer's protocol at a multiplicity of infection of 100 in the presence of 5 μg/ml polybrene (Sigma, St. Louis, MO, USA). In the present study, the lentiviral transfection efficiency was >80%. No significant cell death was observed after viral infection.

Flow cytometric analysis

To assess the expression of various surface markers, mouse and human LR-MSCs were incubated with

fluorescently labeled antibodies at 37 °C for 1 h in the dark followed by two washes with phosphate-buffered saline. Flow cytometry was performed on a FACSCalibur flow cytometer (Becton Dickinson, San Jose, CA, USA), and the data were analyzed using FlowJo software (Tree Star, Ashland, OR, USA). The antibodies used with mouse LR-MSCs included FITC-conjugated anti-stem cell antigen-1 (Sca-1), anti-CD106 and anti-CD34; PE-conjugated anti-CD29, anti-CD44, and anti-CD45; and APC-conjugated anti-CD31. The antibodies used with human LR-MSCs included PE-conjugated anti-CD73, anti-CD44, anti-CD105, anti-HLA-ABC, anti-CD45, anti-CD31, and anti-HLA-DR.

Multilineage differentiation assays

Mouse and human LR-MSCs were seeded at a density of 4×10^3 cells/cm^2 in 12-well plates in standard growth medium and grown to 70% confluence. The osteogenic differentiation potential was evaluated by culturing cells for 3 weeks in osteogenic induction medium, which is basic medium supplemented with 100 nM dexamethasone, 50 μg/ml ascorbic acid, and 10 mM β-glycerophosphate. Then, the deposited calcium phosphate mineral phase was subjected to alizarin red staining. The adipogenic differentiation capacity was confirmed by culturing cells in adipogenic induction medium, which is composed of basic medium, 5 μg/ml insulin, 0.1 μM dexamethasone, 50 μM indomethacin, and 500 μM isobutylmethylxanthine. After 3 weeks, lipid droplets were stained with oil red O solution.

Bleomycin-induced pulmonary fibrosis and treatment

C57BL/6 mice were maintained under specific pathogen-free conditions with free access to water and laboratory rodent chow. Following anesthesia with pentobarbital sodium (3 mg/kg), mice aged 6–7 weeks received a single, slow intratracheal injection of 5 mg/kg bleomycin dissolved in 50 μl of saline with a MicroSprayer (Penn-Century, Wyndmoor, PA, USA). Control mice received 50 μl of saline only. Mice were killed 7, 14, or 21 days after bleomycin instillation.

To investigate the role of the Hh pathway in pulmonary fibrosis, we injected mice with Gant61, a small molecule compound that selectively inhibits Hh signaling [30]. Specifically, 7 days after administration with bleomycin, mice were treated with 25 mg/kg Gant61 or vehicle once daily and were killed on day 14.

To evaluate the effect of Wnt proteins on pulmonary fibrosis, we conducted two animal experiments. In the salinomycin study, mice received a daily intraperitoneal injection of vehicle (10% DMSO/saline) or 5 mg/kg salinomycin, an inhibitor of Wnt/β-catenin signaling that acts on the Wnt/Fzd/LRP complex [31]. In the Wnt10a-knockdown study, mice received intratracheal administration of bleomycin at a dose of 5 mg/kg dissolved in 50 μl of saline. Three days later, 2×10^8 transduction units (TU) of LV-Wnt10a-siRNA or LV-negative control (NC) was administered intratracheally. Mice were killed on day 14 after bleomycin instillation.

Histopathology

Lung tissues were fixed with 4% neutral phosphate-buffered paraformaldehyde overnight, dehydrated, transparentized, and embedded in paraffin before being sectioned into 5-μm-thick slices. Sections were stained with hematoxylin and eosin (H&E) for structural observation, stained with Masson's trichrome/Sirius red for detection of collagen deposits, or subjected to immunohistochemical and immunofluorescence analyses.

Immunohistochemistry

Sections (5 μm thick) were deparaffinized with xylene before rehydration in an ethanol gradient. Next, endogenous peroxidase activity was quenched by incubation with 3% H_2O_2 for 10 min. Sections were then blocked with 3% bovine serum albumin and incubated with rabbit anti-Wnt10a, rabbit anti-Gli1, and goat anti-Gli2 overnight at 4 °C. The primary antibodies were subsequently detected by incubation with horseradish peroxidase-conjugated secondary antibodies (Boster, Wuhan, China) at 37 °C for 1 h. The 3,3′-diaminobenzidine Substrate System (DAKO, Glostrup, Denmark) was used to reveal the immunohistochemical staining.

Immunofluorescence

Immunofluorescence analyses of LR-MSCs and lung tissues were performed as described previously [32]. The following primary antibodies were employed: rabbit anti-Wnt10a, rat anti-Sca-1, mouse anti-α-smooth muscle actin (α-SMA), and rabbit anti-collagen I. Alexa Fluor 594-conjugated goat anti-rabbit antibody, Alexa Fluor 488-conjugated goat anti-mouse antibody, and Alexa Fluor 647-conjugated goat anti-rat antibody (all from Invitrogen) were used as secondary antibodies. Nuclei were stained with 2 mg/ml 4′,6-diamidino-2-phenylindole (Sigma). Images were acquired using a confocal fluorescence microscope (Olympus, Tokyo, Japan).

Quantitative real-time polymerase chain reaction (qRT-PCR)

Total RNA was extracted from cultured cells or lung tissues using Trizol reagent (Invitrogen) according to the manufacturer's instructions. qRT-PCR was conducted by amplifying 20 μl of diluted cDNA with a SYBR Green qRT-PCR kit (Roche, Mannheim, Germany) using a 7300 Real-time PCR System (Applied Biosystems, Waltham, MA, USA). The relative quantification of target gene expression was performed using glyceraldehyde-3-phosphate dehydrogenase (GAPDH) mRNA as the internal control. The sequences of the primer pairs used in this study are listed in Supplementary Table 2.

Western blot

Proteins were purified from either lung tissues or LR-MSCs. Cytosolic and nuclear fractions were prepared with cytoplasmic and nuclear extraction kits (Invent Biotechnologies, Eden Prairie, MN, USA) according to the manufacturer's instructions. Briefly, proteins were separated on sodium dodecyl sulfate-polyacrylamide gels and then electrophoretically transferred to polyvinylidene difluoride membranes. Next, membranes were blocked with 5% nonfat milk and incubated with specific primary antibodies, including mouse anti-α-SMA, rabbit anti-collagen I, rabbit anti-fibronectin, rabbit anti-Wnt10a, rabbit anti-phospho (p)-β-catenin, rabbit anti-β-catenin, rat anti-Shh, rabbit anti-Gli1, goat anti-Gli2, rabbit anti-Ptc, rabbit anti-Sca-1, rabbit anti-Lamin B and rabbit anti-GAPDH. Species-matched horseradish peroxidase-conjugated IgG was used as the secondary antibody. Immunoreactive protein bands were detected using an Odyssey Scanning System (LI-COR, Lincoln, NE, USA). The expression levels of proteins were quantified by densitometry using ImageJ (NIH, Bethesda, MD, USA) and normalized to the expression of GAPDH.

Chromatin immunoprecipitation (ChIP)

The transcription factor Gli1 is predicted to regulate the transcription of the Wnt10a gene; thus, we examined its binding with the Wnt10a promoter using a ChIP assay kit (Thermo, Rockford, IL, USA) according to the manufacturer's instructions. Mouse LR-MSCs were subjected to crosslinking with 1% formaldehyde. After the reaction was terminated with 0.1 M glycine, chromatin was sheared into fragments of 500–1000 bp in length. DNA immunoprecipitated with anti-Gli1 was subjected to RT-PCR. Wnt10a promoter-specific primers were used to amplify the Gli1 binding regions. The primers used were as follows: Wnt10a promoter sense, 5′-GCTGCATATCCCAGGCTT-3′ and Wnt10a promoter antisense, 5-GGTGCCCACAGGAACAGG-3′.

Statistical analysis

The data were analyzed for statistical significance with SPSS 18.0 (SPSS, Chicago, IL, USA) and are presented as the means ± SD. Paired comparisons were performed using Student's *t*-test, and differences among groups were analyzed by one-way analysis of variance (ANOVA). Significance was accepted when p was <0.05.

Results

Wnt10a is upregulated in the lungs of bleomycin-treated mice

Following intratracheal instillation of bleomycin, the alveolar structure was destroyed, and collagen deposition began in mouse lungs from days 7 to 21, as assessed by H&E and Masson's trichrome staining (Fig. 1a). Recent studies demonstrated the activation of Wnt signaling and increased expression of several Wnt family members in IPF, suggesting a role for this pathway in the development of pulmonary fibrosis [33, 34]. Here, a comprehensive survey of the mRNA levels of all 19 Wnts revealed a marked induction of Wnt10a in lungs after bleomycin administration (Fig. 1b). Relative to saline control lungs, fibrotic lungs exhibited elevated protein levels of Wnt10a and the fibrosis markers α-SMA, collagen I, and fibronectin (Fig. 1c). Upregulation of Wnt10a in the lungs of bleomycin-treated mice was further confirmed by immunohistochemistry (Fig. 1d, e). Moreover, nuclear translocation of p-β-catenin was induced in the bleomycin mouse model, indicating the activation of canonical Wnt signaling during pulmonary fibrosis (Fig. 1f).

Wnt10a is highly expressed in LR-MSCs undergoing myofibroblastic differentiation

As the level of Wnt10a was markedly increased after bleomycin treatment, we next clarified the source of its production. Accumulating evidence indicates that lung tissue contains a population of LR-MSCs that are precursors of myofibroblasts [7]. This observation prompted us to conduct a fate-tracing experiment to determine whether LR-MSCs play a role during pulmonary fibrosis. Here, we observed an expansion of the LR-MSC population in fibrotic lesions, where these cells differentiated into α-SMA$^+$ myofibroblasts (Fig. 2a). MSCs have been reported to regulate fibroblast growth and collagen production by secreting autocrine or paracrine factors, such

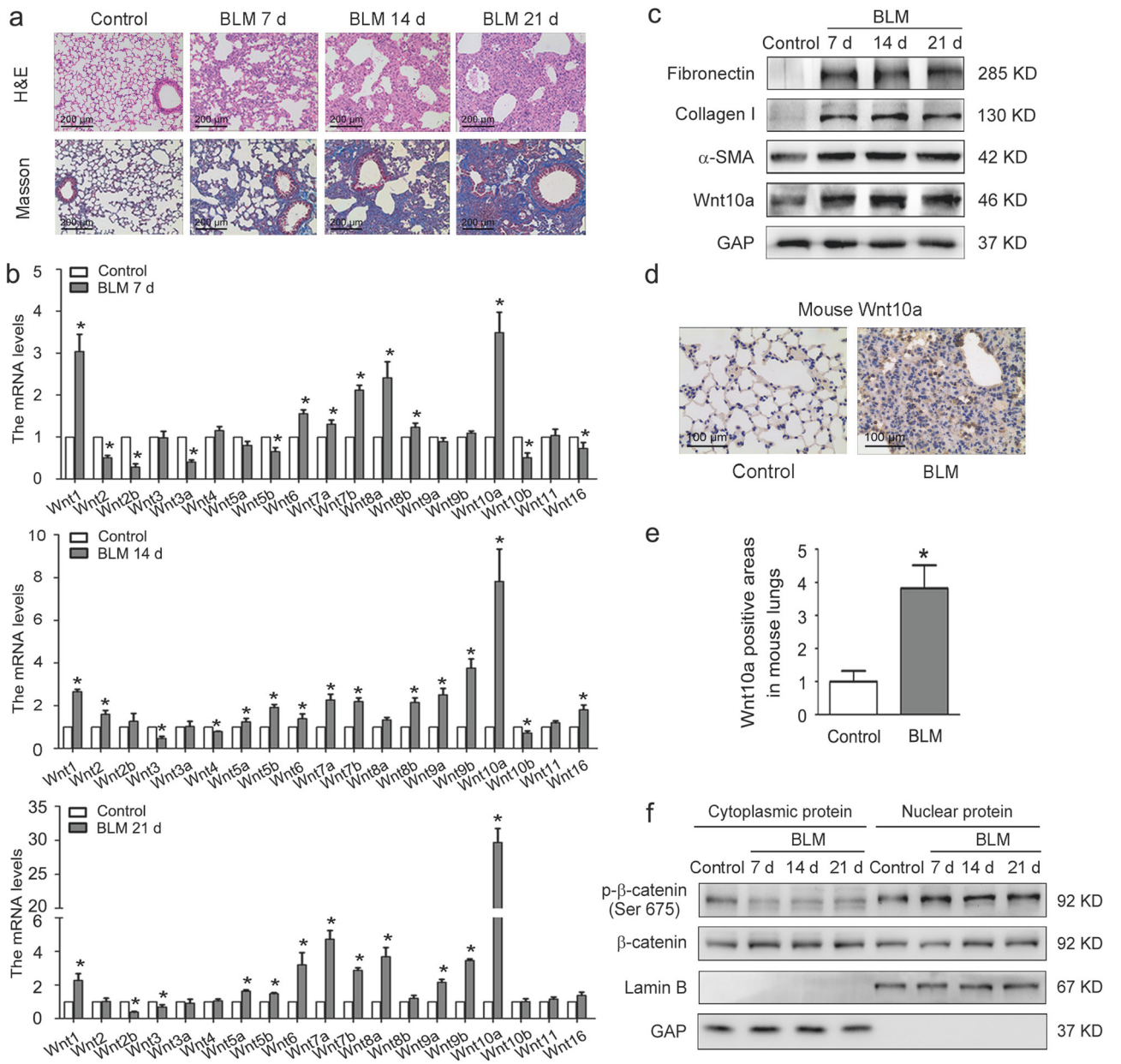

Fig. 1 Wnt10a is induced in the bleomycin mouse model. Mice ($n = 6$ per group) received either saline or bleomycin (BLM) (5 mg/kg body weight) intratracheally and were killed 7, 14, or 21 days (d) later and their lung tissues were analyzed. **a** Pulmonary fibrotic lesions were determined by hematoxylin-eosin (H&E) and Masson's trichrome staining. **b** The mRNA levels of 19 Wnt genes were determined by qRT-PCR. The results are shown as the means ± SD (*$P < 0.05$ versus control). **c** The expression of fibronectin, collagen I, α-smooth muscle actin (α-SMA), and Wnt10a was measured by western blot. **d** Wnt10a expression in lung sections from control and BLM-treated mice was analyzed by immunohistochemistry. **e** The percentages of $Wnt10a^+$ areas were quantified (*$P < 0.05$ versus control). **f** Cytoplasmic and nuclear extracts were prepared and analyzed by western blot using anti-p-β-catenin and anti-β-catenin antibodies. Lamin B and glyceraldehyde-3-phosphate dehydrogenase (GAPDH) were used as the loading controls for nuclear and cytoplasmic proteins, respectively

as Wnt proteins [10]. Our dual immunofluorescence analyses showed localization of some Wnt10a in LR-MSCs that coexpressed the stem cell marker Sca-1 and the myofibroblast marker α-SMA (Fig. 2b), consistent with the concept that the myofibroblastic differentiation of LR-MSCs during pulmonary fibrosis is likely to proceed via Wnt signaling [12, 13].

To further explore the underlying correlation between LR-MSCs and Wnt10a in the pathogenesis of pulmonary fibrosis, we isolated primary LR-MSCs from mouse lung tissues. These cells, with a long spindle shape and a spiral, radial arrangement, demonstrated a typical mouse MSC surface marker profile positive for Sca-1, CD29, CD106 and CD44 but negative for CD45, CD34, and CD31

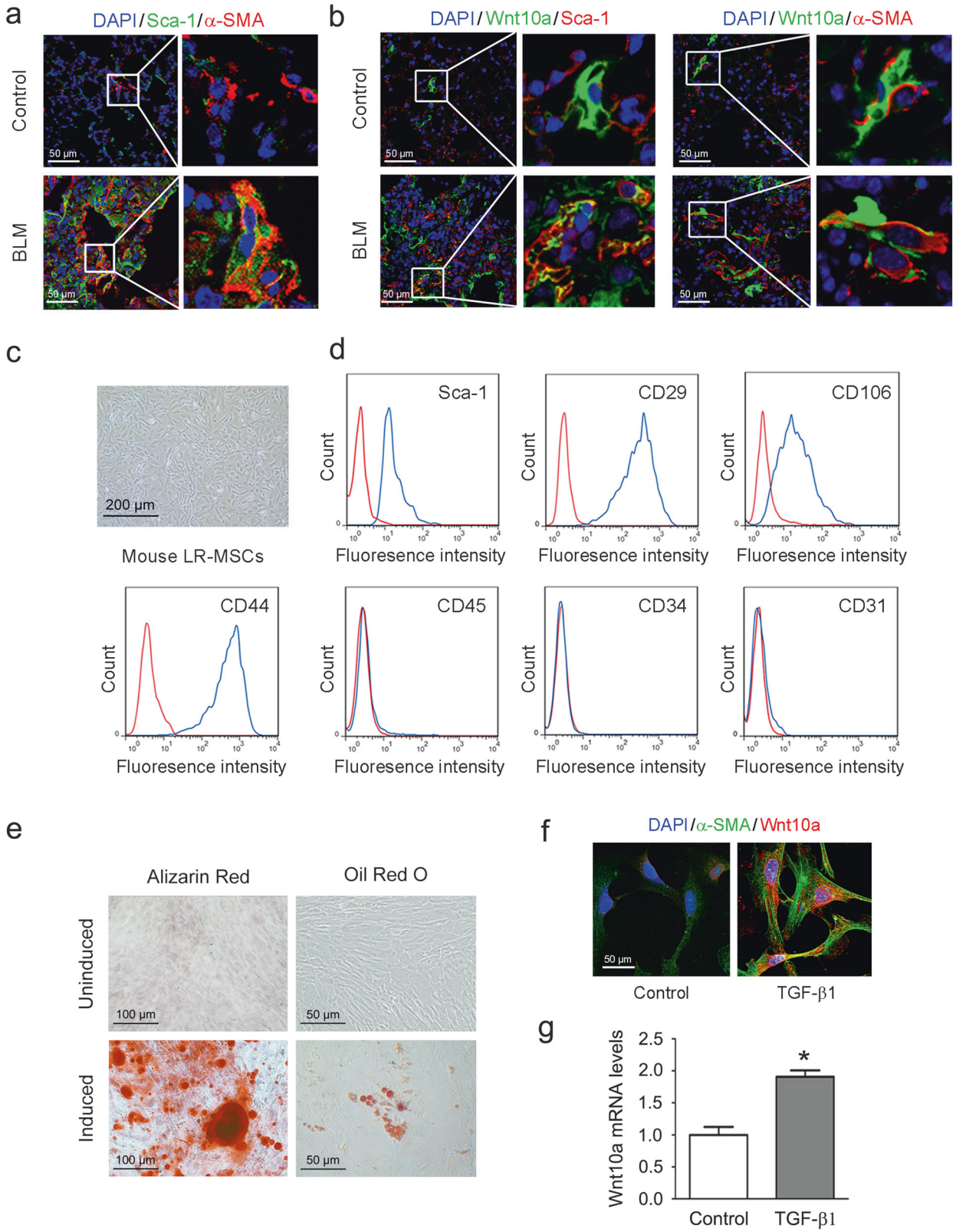
a
DAPI/Sca-1/α-SMA
Control
BLM
50 μm
b
DAPI/Wnt10a/Sca-1
DAPI/Wnt10a/α-SMA
c
200 μm
Mouse LR-MSCs
d
Sca-1
CD29
CD106
CD44
CD45
CD34
CD31
Count
Fluoresence intensity
e
Alizarin Red
Oil Red O
Uninduced
Induced
100 μm
50 μm
f
DAPI/α-SMA/Wnt10a
Control
TGF-β1
g
Wnt10a mRNA levels
2.5
2.0
1.5
1.0
0.5
0.0
*
Control
TGF-β1

◀ **Fig. 2** Wnt10a is upregulated during LR-MSC-to-myofibroblast transition. **a**, **b** Mice ($n = 6$ per group) received either saline or bleomycin (BLM) (5 mg/kg body weight) intratracheally and were killed on day 14. **a** Myofibroblastic differentiation of lung-resident mesenchymal stem cells (LR-MSCs) in mouse lung tissues was analyzed using a dual immunofluorescence assay to detect the expression of stem cell antigen-1 (Sca-1) and α-smooth muscle actin (α-SMA). **b** Colocalization of Wnt10a and Sca-1 or α-SMA in mouse lung tissues was determined by immunofluorescence. **c–g** Mouse LR-MSCs were isolated from the lungs of naive mice using magnetic-activated cell sorting (MACS) and cultured for 7 days. **c** Cell morphology was revealed by conventional light microscopy. **d** Cell surface markers were analyzed by flow cytometric analysis. Red line, isotype control; Blue line, respective surface marker staining. **e** Mouse LR-MSCs were seeded in the appropriate differentiation induction medium. After a 21-day osteogenic or adipogenic differentiation period, cells were stained with alizarin red to assess the accumulation of matrix mineralization or with oil red O to detect the formation of lipid droplets. Mouse LR-MSCs were treated with 10 ng/ml transforming growth factor-β1 (TGF-β1) for 48 h followed by the measurement of the expression of α-SMA and Wnt10a using immunofluorescence (**f**) and the measurement of the mRNA levels of Wnt10a using qRT-PCR (**g**). The results are shown as the means ± SD (*$P < 0.05$ versus control)

(Fig. 2c, d). Combining these findings with capacity of these cells to differentiate towards osteocytes and adipocytes, we confirmed that this cell population possessed the main features of MSCs (Fig. 2e). Cultured mouse LR-MSCs were then activated by transforming growth factor-β1 (TGF-β1), displaying upregulation of Wnt10a and the formation of α-SMA$^+$ stress fibers (Fig. 2f). The mRNA level of Wnt10a was also elevated during this transdifferentiation process (Fig. 2g). These results suggested that the Wnt10a highly expressed during pulmonary fibrosis might be secreted by LR-MSCs undergoing myofibroblastic activation.

LR-MSCs undergoing myofibroblastic differentiation during pulmonary fibrotic events are Hh responsive

A previous study indicated that the Hh pathway interacts with Wnts to maintain the quiescence of stem cells and orchestrate tissue homeostasis [35]. Considering the crosstalk between Hh signaling and Wnt proteins, we evaluated the functional role of the Shh pathway in pulmonary fibrogenesis. After bleomycin injury, Shh expression was induced in the lungs of rodents (Fig. 3a). Along with upregulation of Hh ligands, nuclear translocation of the downstream effectors Gli1 and Gli2 was facilitated (Supplementary Fig. 1). Preferential nuclear localization of Gli proteins in the bleomycin mouse model was also found by immunohistochemical staining, supporting the role of these proteins as transcription factors in this pathway (Fig. 3b).

The Shh signaling has been shown to regulate the differentiation of various types of cells into myofibroblasts; this transdifferentiation occurs in MSCs during fibrosis in many organs, including the lung [22, 36]. To explore the activity of Shh signaling in LR-MSCs during pulmonary fibrosis, we isolated LR-MSCs from control and bleomycin-treated mice. Intratracheal bleomycin exposure markedly elevated the expression of myofibroblast markers in LR-MSCs (Fig. 3c). Notably, LR-MSCs from bleomycin-treated mice expressed higher levels of the Hh signaling components Shh, Gli1, and Gli2 but a lower level of the negative regulatory receptor Ptc than LR-MSCs from sham-operated controls (Fig. 3d). These results indicated that LR-MSCs undergoing myofibroblastic differentiation were the targets of the Shh pathway during pulmonary fibrosis. Consistent with the in vivo finding, the Shh/Gli signaling cascade was activated in LR-MSCs treated with TGF-β1 (Fig. 3e).

To further confirm that LR-MSCs-undergoing myofibroblastic transition are Hh responsive, we incubated cells with various concentrations of recombinant Shh. As expected, these cells responded to Shh stimulation, displaying dose-dependent nuclear translocation of Gli (Fig. 3f). Moreover, differentiation of LR-MSCs into myofibroblasts was found following Shh stimulation, suggesting the regulatory effect of the Shh pathway on LR-MSC fibrogenic activity (Fig. 3g, Supplementary Fig. 2).

The Shh pathway regulates myofibroblastic activation of LR-MSCs and pulmonary fibrosis via Wnt/β-catenin signaling

Given the critical role of Shh signaling in LR-MSC-to-myofibroblast transition and pulmonary fibrosis, we next evaluated whether inhibition of Gli, the final effectors of the Hh pathway, could retard fibrotic progression. Gant61, a small molecule compound directly blocking the binding of Gli to DNA targets, was selected for Shh pathway suppression [30]. As seen by histopathology and morphometry, Gant61 treatment from day 7 to 14 after bleomycin administration reduced the severity of pulmonary fibrotic lesions (Fig. 4a). Administration of Gant61 attenuated the mRNA levels of fibroblast-specific protein-1 and fibronectin, two fibrogenic genes associated with ECM deposition (Fig. 4b). In addition, bleomycin-induced expression of α-SMA, collagen I and fibronectin was inhibited, along with the suppression of LR-MSC marker Sca-1, indicating that reduced transdifferentiation of LR-MSCs contributed to the decrease in myofibroblast formation in pulmonary fibrosis (Fig. 4c). Gant61 was also found to abolish TGF-β1-induced fibrogenic activity in vitro, confirming the role of the Hh pathway in LR-MSC-to-myofibroblast transition (Fig. 4d).

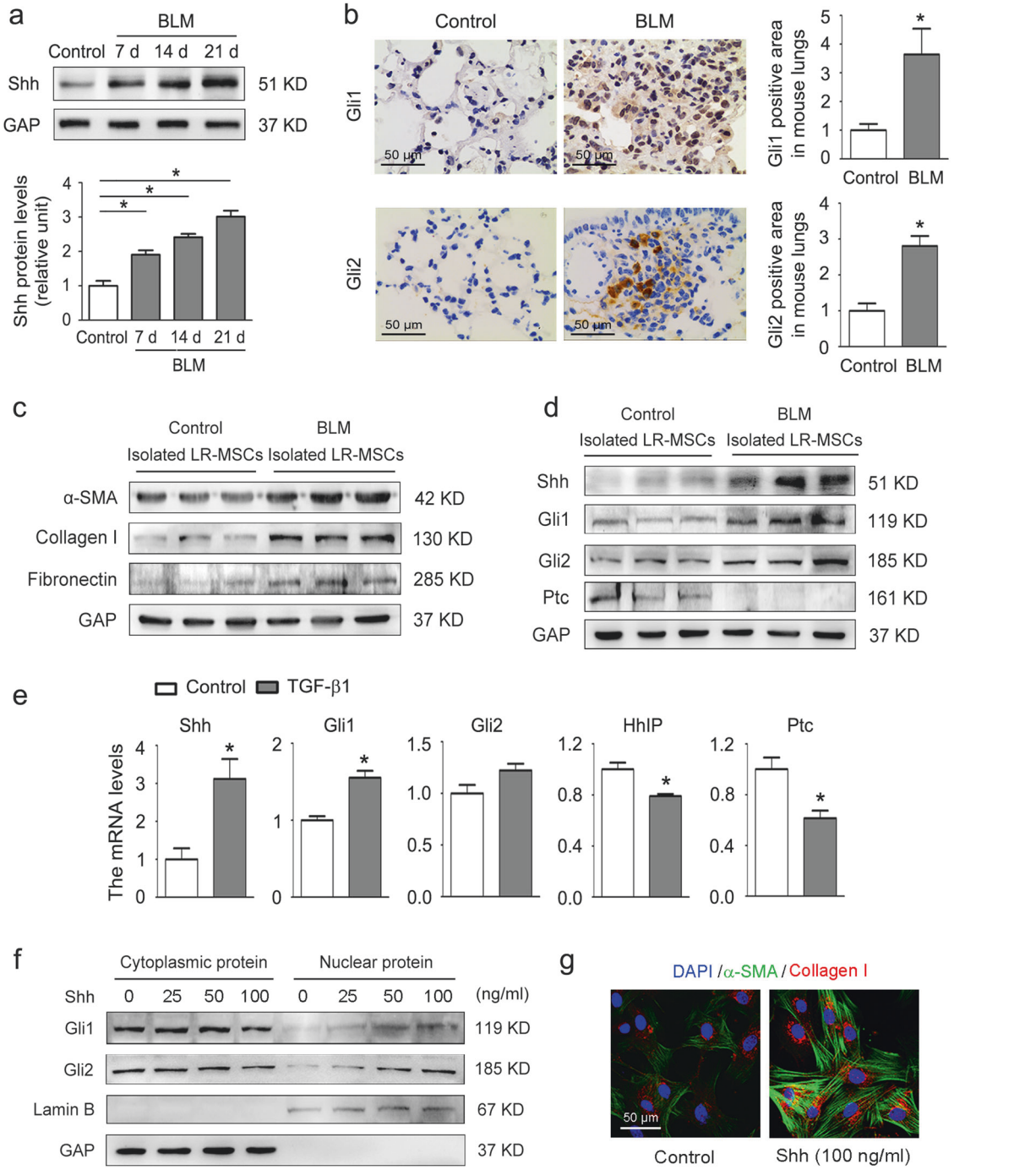

Fig. 3 Sonic hedgehog pathway activity increases in LR-MSCs after bleomycin administration in mice. **a–d** Mice ($n = 6$ per group) received either saline or bleomycin (BLM) (5 mg/kg body weight) intratracheally and were killed 7, 14, or 21 days (d) later. **a** The expression of the sonic hedgehog (Shh) in mouse lung tissues was examined by western blot. The expression levels of Shh were quantified by densitometry with normalization to the expression of glyceraldehyde-3-phosphate dehydrogenase (GAPDH). **b** The expression of glioblastoma1 (Gli1) and Gli2 in lung sections from control and BLM-treated mice was analyzed by immunohistochemistry. The percentages of $Gli1^+$ or $Gli2^+$ areas were quantified (*$P <$ 0.05 versus control). The protein levels of myofibroblast markers (**c**) and shh signaling components (**d**) in lung-resident mesenchymal stem cells (LR-MSCs) isolated from BLM-treated mice or sham-operated controls were measured by western blot. **e** The mRNA levels of Shh pathway components in mouse LR-MSCs treated with 10 ng/ml transforming growth factor-β1 (TGF-β1) for 48 h were analyzed by qRT-PCR. The results are shown as the means ± SD (*$P < 0.05$ versus control). **f** Cytoplasmic and nuclear expression of Gli in mouse LR-MSCs treated with various concentrations of recombinant Shh as indicated for 48 h were assessed by western blot. Lamin B was used as the nuclear internal control, and GAPDH was used as the cytoplasmic internal control. **g** The expression of α-smooth muscle actin (α-SMA) and collagen I in mouse LR-MSCs treated with 100 ng/ml recombinant Shh for 48 h was analyzed by immunofluorescence

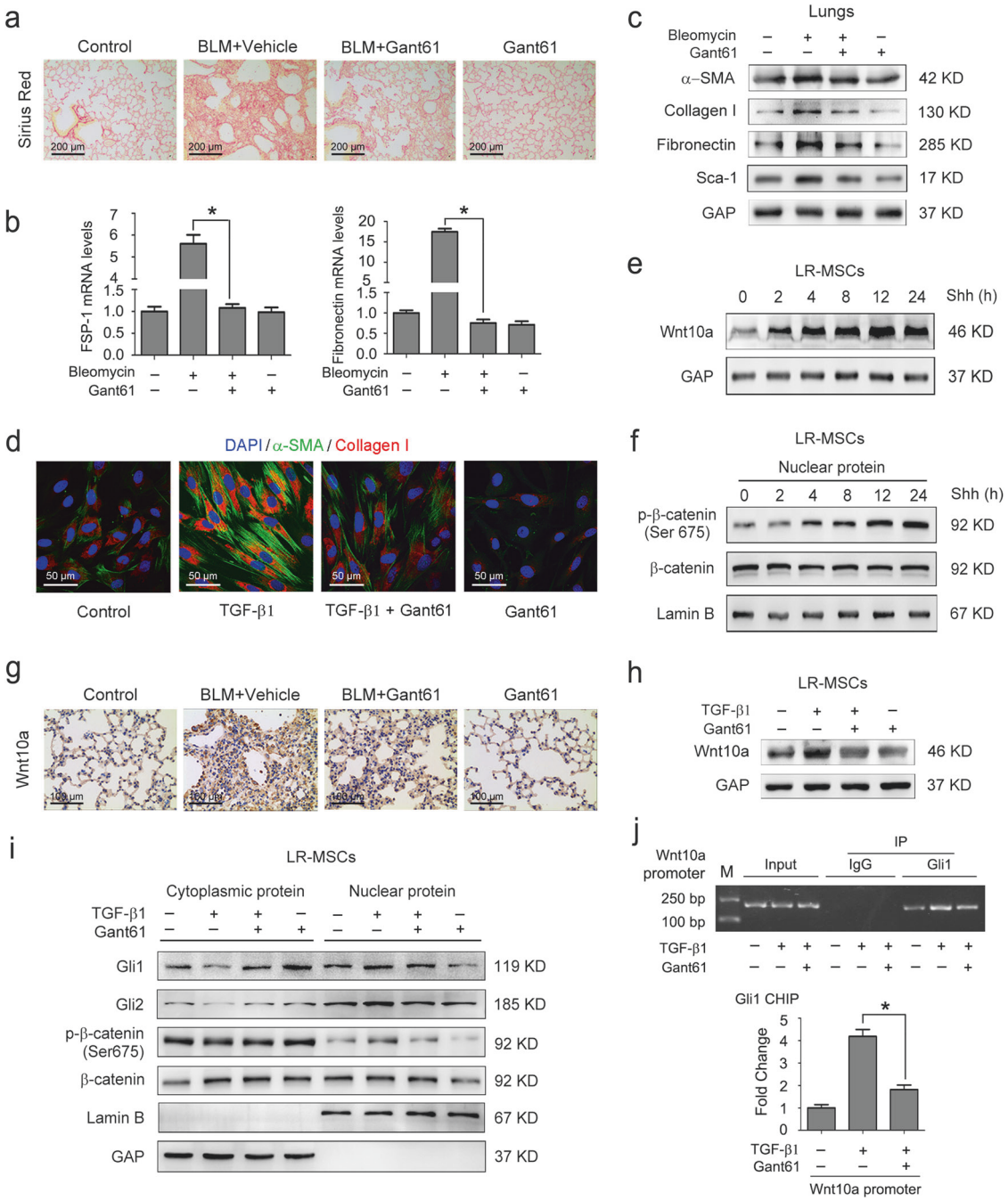

Crosstalk between Wnt signaling and the Shh/Gli system machinery has been implicated in stem cell differentiation. Therefore, we aimed to clarify the relationship between these two pathways. Here, Wnt10a expression was induced in cultured LR-MSCs at 2 h after incubation with Shh and was sustained to 24 h (Fig. 4e). Shh addition also increased the nuclear protein levels of p-β-catenin in a time-dependent manner (Fig. 4f). Intriguingly, nuclear translocation of p-β-catenin lagged behind Wnt10a induction, consistent with the downstream position of β-catenin with respect to Wnt ligands. In the intervention experiment, blockade of Gli disrupted Wnt signaling activation by impairing the upregulation of Wnt10a and nuclear translocation of p-β-catenin (Fig. 4g–i, Supplementary Fig. 3). To delineate the regulatory mechanism of the Hh pathway involved in the Wnt signaling, we performed a ChIP assay. The ChIP results revealed increased occupancy of Gli1 at the promoter regions of Wnt10a in response to TGF-β1, which was reversed by prior treatment with Gant61 (Fig. 4j).

◀ **Fig. 4** The sonic hedgehog pathway regulates pulmonary fibrotic events via Wnt/β-catenin signaling. **a–c** Mice ($n = 6$ per group) were intraperitoneally injected with vehicle (10% DMSO/saline) or 25 mg/kg Gant61 three times weekly as indicated 7 days after bleomycin (BLM) administration. Mice were killed on day 14 after BLM instillation. **a** Collagen deposition in mouse lung tissues was revealed by Sirius red staining. **b** The mRNA levels of fibroblast-specific protein-1 (FSP-1) and fibronectin in mouse lung tissues were determined by qRT-PCR. The results are shown as the means ± SD (*$P < 0.05$ versus BLM + vehicle). **c** The protein levels of α-smooth muscle actin (α-SMA), collagen I, fibronectin, and stem cell antigen-1 (Sca-1) in mouse lung tissues were measured by western blot. **d** Mouse lung-resident mesenchymal stem cells (LR-MSCs) were pretreated with 5 μM Gant61 for 1 h followed by stimulation with 10 ng/ml transforming growth factor-β1 (TGF-β1) for 48 h. The expression of α-SMA and collagen I in mouse LR-MSCs was examined by immunofluorescence. Mouse LR-MSCs were incubated with 100 ng/ml recombinant sonic hedgehog (Shh) for various durations as indicated, and the expression of Wnt10a (**e**) and nuclear translocation of p-β-catenin and β-catenin (**f**) were analyzed by western blot. Lamin B was used as the nuclear marker. **g** Mice were treated as described in **a**–**c**. Wnt10a expression in mouse lung tissues was analyzed by immunohistochemistry. **h–j** Mouse LR-MSCs were treated as described in **d**. **h** The protein levels of Wnt10a in mouse LR-MSCs were measured by western blot. **i** Cytoplasmic and nuclear expression of glioblastoma1 (Gli1), Gli2, p-β-catenin, and β-catenin in mouse LR-MSCs were determined by western blot. Lamin B and glyceraldehyde-3-phosphate dehydrogenase (GAPDH) were used as the loading controls for nuclear and cytoplasmic proteins, respectively. **j** The association of Gli1 with the Wnt10a promoter region in mouse LR-MSCs was analyzed by chromatin immunoprecipitation (ChIP). Normal mouse IgG was used as the control antibody. A representative gel image is shown, and the expression levels were quantified by densitometry and normalized to the input. The results are shown as the means ± SD (*$P < 0.05$ versus TGF-β1)

Inhibition of Wnt proteins exerts an antifibrotic effect in activated LR-MSCs and bleomycin-injured lungs

We screened Wnt family members in the bleomycin mouse model and found that the Wnt10a released from activated LR-MSCs might be a factor affecting pulmonary fibrosis. As a ligand in canonical Wnt signaling, Wnt10a binds with the Fzd/LRP receptor to activate downstream β-catenin. Thus, we used a small molecule compound, salinomycin, to investigate the effect of the Wnt/Fzd/LRP complex on pulmonary fibrotic events [31]. As expected, salinomycin treatment suppressed canonical Wnt signaling activity, as evidenced by the decreased nuclear translocation of p-β-catenin (Fig. 5a). Notably, injection of salinomycin protected mice from bleomycin-induced pulmonary fibrosis with a decline in the LR-MSC population (Fig. 5b, c). Our in vitro data confirmed that the transformation of LR-MSCs into pathological myofibroblasts was inhibited by salinomycin (Fig. 5d).

To better understand the role of Wnt10a in pulmonary fibrosis, we intratracheally administered LV-Wnt10a-siRNA to mice. On day 14, Wnt10a-knockdown mice exhibited alleviated pulmonary fibrosis, as determined by histological analysis (Fig. 5e, Supplementary Fig. 4a). In addition, silencing Wnt10a suppressed the induction of the LR-MSC antigen Sca-1 and fibrosis markers and reduced the nuclear translocation of p-β-catenin in bleomycin-treated mice (Fig. 5f, g). Similarly, downregulation of Wnt10a impaired TGF-β1-elicited nuclear expression of p-β-catenin and myofibroblastic activation of LR-MSCs (Fig. 5h, i, Supplementary Fig. 4b). We further confirmed the suppressive effect of LV-Wnt10a-siRNA on the acquisition of the aggressive profibrotic phenotype in LR-MSCs by immunofluorescence staining (Fig. 5j). Together, these results demonstrated that inhibition of Wnt proteins efficiently ameliorated pulmonary fibrotic events in mice.

Induction of Wnt10a expression and activation of the Shh/Gli signaling cascade are involved in human pulmonary fibrosis

To verify our findings in a clinical setting, we extended our mouse experiments to human samples. As shown in Fig. 6a, a high level of Wnt10a was found in the lungs of IPF patients. We observed positive Wnt10a staining in LR-MSCs undergoing transition from a Sca-1-expressing stem cell phenotype to an α-SMA-expressing myofibroblast phenotype during human pulmonary fibrosis (Fig. 6b, c). Next, human LR-MSCs were isolated from the distal lungs of patients undergoing pneumonectomy for pneumothorax. Similar to other tissue MSCs, this cell population with a long, thin, stellate morphology showed a typical MSC surface marker profile and possessed the capacity to differentiate towards osteoblasts and adipocytes (Supplementary Fig. 5). Cultured human LR-MSCs were then induced to transdifferentiate into α-SMA$^+$ myofibroblasts under stimulation with human TGF-β1. Along with myofibroblastic differentiation, increased expression of Wnt10a was observed in human LR-MSCs (Fig. 6d, e). Furthermore, we found upregulation of Shh, Gli1 and Gli2 and downregulation of Hhip and Ptc during human LR-MSC-to-myofibroblast transition, suggesting a role for the Shh pathway in human pulmonary fibrotic events (Fig. 6f).

Discussion

IPF is a progressive, fatal illness characterized by altered cellular composition and homeostasis in the lungs [37]. During the past few decades, several signaling pathways underlying pulmonary fibrosis have been described. We and others have previously evaluated the effect of canonical Wnt signaling on the development of experimental pulmonary fibrosis [13, 38]. In this study, we linked canonical Hh signaling with Wnt10a expression to demonstrate a

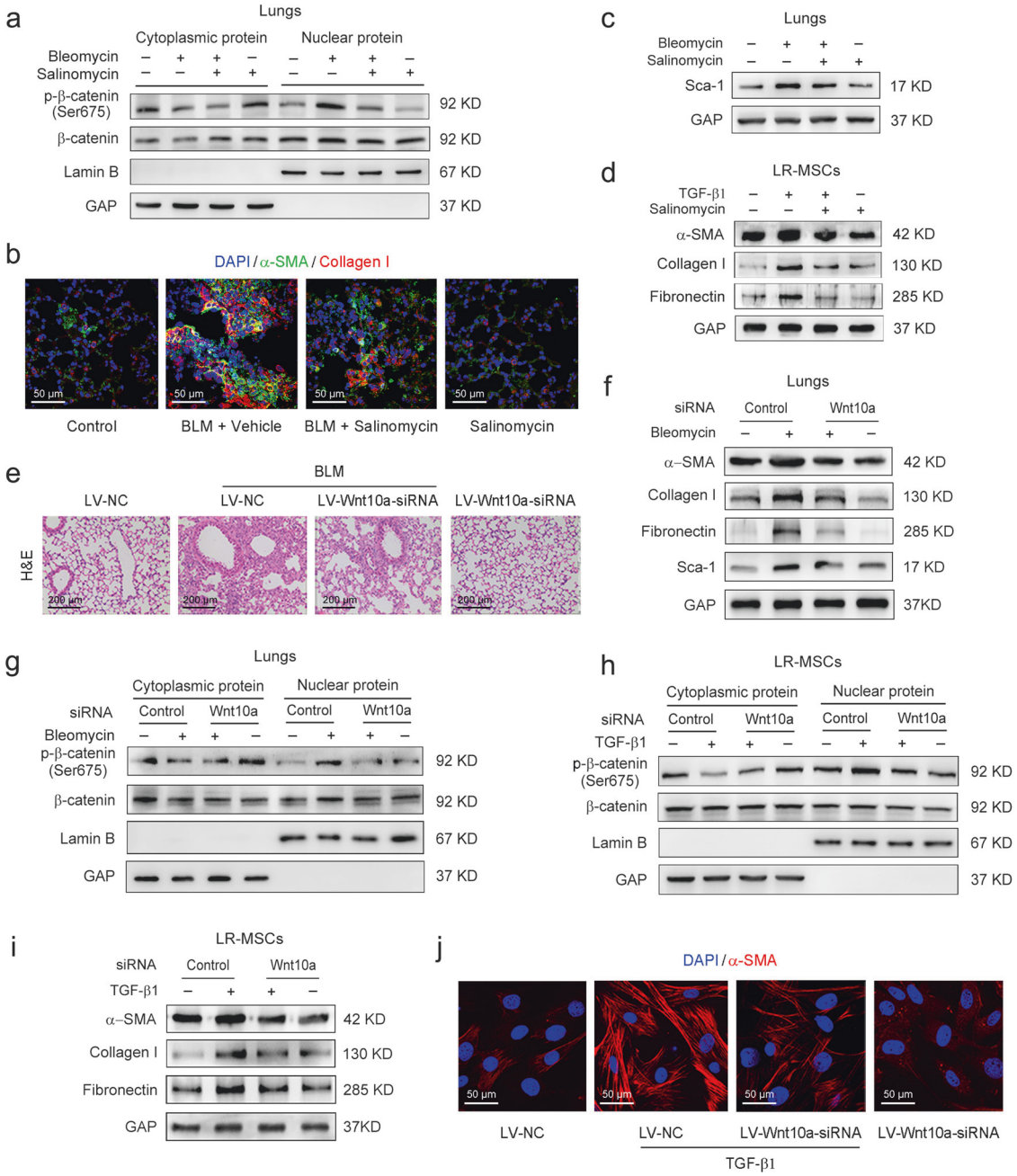

mechanism by which LR-MSCs participate in the development of pulmonary fibrosis (Fig. 7). First, we performed a systematic analysis of the mRNA levels of 19 Wnt genes in the lungs of bleomycin-treated mice. Most Wnt family members, especially Wnt10a, were induced in this model of pulmonary fibrosis, supporting the idea that the Wnt pathway mediated by Wnt ligands is activated in IPF [33]. Our observation in lung tissues is consistent with the acknowledged actions of Wnt molecules in other systems. For example, after unilateral ureteral obstruction, all members of the Wnt family except Wnt5b, Wnt8b, and Wnt9b are upregulated in the fibrotic kidneys with distinct dynamics [39]. In addition, increased expression of several Wnt genes, such as Wnt2, Wnt9a, Wnt10b, and Wnt11, is observed in the skin of tight skin mice, an animal model of systemic sclerosis [40].

Activation of α-SMA$^+$ myofibroblasts is arguably the central event in IPF [37]. However, no single marker can reliably distinguish myofibroblasts from other cell types such as fibroblasts, smooth muscle cells and pericytes. The marker α-SMA, especially when expressed at a high level, remains a widely recognized marker of myofibroblasts [41]. Accumulating evidence indicates that lung tissues contain a population of endogenous MSCs, which can be triggered by local factors

◀ **Fig. 5** Blockade of Wnt proteins attenuates myofibroblastic differentiation of LR-MSCs and pulmonary fibrosis. **a–c** Mice ($n = 6$ per group) were intraperitoneally injected with vehicle (10% DMSO/saline) or 5 mg/kg salinomycin every other day as indicated 7 days after bleomycin (BLM) instillation. Mice were killed on day 14 after BLM administration. **a** Cytoplasmic and nuclear extracts were prepared and analyzed by western blot using anti-p-β-catenin and anti-β-catenin antibodies. Lamin B was used as the nuclear internal control, and glyceraldehyde-3-phosphate dehydrogenase (GAPDH) was used as the cytoplasmic internal control. **b** The expression of α-smooth muscle actin (α-SMA) and collagen I in mouse lung tissues was analyzed by immunofluorescence. **c** The protein levels of stem cell antigen-1 (Sca-1) in mouse lung tissues were determined by western blot. **d** Mouse lung-resident mesenchymal stem cells (LR-MSCs) were pretreated with 1 μM salinomycin for 1 h followed by stimulation with 10 ng/ml transforming growth factor-β1 (TGF-β1) for 48 h. The expression of α-SMA, collagen I and fibronectin was examined by western blot. **e–g** Mice ($n = 6$ per group) received either LV-negative control (NC) or LV-Wnt10a-siRNA (2×10^8 TU in 50 μl of saline) intratracheally on day 3 after BLM instillation. Mice were killed 14 days after BLM administration. **e** The effect of LV-Wnt10a-siRNA on pulmonary fibrotic lesions was determined by hematoxylin-eosin (H&E) staining. **f** The expression of the fibrosis markers and Sca-1 in mouse lung tissues was measured by western blot. **g** Cytoplasmic and nuclear extracts were prepared and analyzed by western blot using anti-p-β-catenin and anti-β-catenin antibodies. Lamin B and GAPDH were used as the nuclear and cytosolic markers, respectively. **h–j** Mouse LR-MSCs were transfected with LV-NC or LV-Wnt10a-siRNA in the presence or absence of 10 ng/ml TGF-β1 followed by incubation for 48 h. **h** The expression of p-β-catenin and β-catenin in the cytoplasm and nucleus was examined by western blot. Lamin B and GAPDH were used as the loading controls for nuclear and cytoplasmic proteins, respectively. **i** The protein levels of the fibrosis markers in mouse LR-MSCs were measured by western blot. **j** The expression of α-SMA in mouse LR-MSCs was analyzed by immunofluorescence

to differentiate into myofibroblasts that participate in fibrosis progression [11]. Our fate-tracing assay in a murine model of pulmonary fibrosis showed these pathophysiological events. These resident MSCs mediate pathogenic processes largely through the secretion of proscarring, proangiogenic, and immunomodulatory factors [10]. As Wnt signaling has been suggested to play a critical role in MSC fate decisions, Wnt ligands may be expressed in this type of cell. Indeed, we observed localization of Wnt10a expression in LR-MSCs undergoing myofibroblastic activation in fibrotic lungs and found an increase in Wnt10a expression during LR-MSC-to-myofibroblast transition in vitro. These results are consistent with the concept that secreted Wnt proteins remain associated with the cell surface or ECM where they are produced and are further involved in subsequent autocrine or paracrine signal transduction [42].

The expression of Wnts is reported to be regulated by the Shh pathway, an evolutionarily conserved signaling cascade governing tissue patterning and stem cell differentiation. As blood vessel walls are the in vivo niches of MSCs, primary LR-MSCs were isolated from the lungs of bleomycin-treated mice, where they exhibited the myofibroblast phenotype and high Shh pathway activity. These characteristics defined LR-MSCs as the Shh-responsive cells in pulmonary fibrosis. Therefore, recombinant Shh stimulation was sufficient to promote myofibroblastic differentiation of LR-MSCs, whereas Gant61 treatment could attenuate LR-MSC-to-myofibroblast transition and pulmonary fibrosis. During the formation of initial lung buds, paracrine activity of Shh via mesenchymal Gli2/3 is required for the expression of Wnt2/2b [43]. Consistent with the effect of Shh/Gli signaling cascade on Wnt pathway during lung development, the expression of Wnt10a and nuclear translocation of p-β-catenin during pulmonary fibrotic events were induced under Shh stimulation while reduced with Gant61 treatment, suggesting a multilevel interaction between these two pathways. Moreover, factors in addition to the Shh-Wnt signaling may be involved in the regulation of myofibroblastic differentiation. For example, serum response factor (SRF) and its coactivator myocardin-regulated transcription factor A (MRTF-A) are two known master regulators of α-SMA. A previous study demonstrated that β-catenin can physically associate with the promoter of MRTF-A to promote MRTF-A transcription and can dramatically impact the association of SRF with MRTF-A [44, 45]. Considering the influence of multiple transcription factors in pulmonary fibrosis, it is not surprising that the expression of fibrosis markers such as α-SMA may not be completely consistent with the expression of Wnt10a.

Biomarkers investigated in fibrotic diseases reflect and broaden the current understanding of the events underlying tissue scarring. Recently, Wnt10a overexpression was shown to be associated with an increased risk of mortality in patients with acute exacerbation of IPF and was thus identified as a sensitive predictor for IPF [46]. As a target of miR-378a-3p, Wnt10a is involved in the effect of miR-378a-3p on hepatic stellate cell activation. Silencing Wnt10a blocks the contribution of the miR-378a-3p inhibitor to the activation of hepatic stellate cells [47]. Here, we confirmed the contribution of Wnt10a inhibition to the maintenance of LR-MSC quiescence and protection of mice from pulmonary fibrosis. However, the comparison between Gli blockade and Wnt inhibition in terms of antifibrotic efficacy and side effects remains to be clarified in future studies. Moreover, the means by which Wnt signaling elicits a biological response largely depends on the combination of Wnt ligands with the corresponding receptors that are present. According to a systematic analysis of Fzd receptor expression in a previous report, the expression levels of Fzd9 and Fzd10 are dramatically increased in both TGF-β-treated LR-MSCs and bleomycin-injured lungs. As a ligand, Wnt10a operates via binding to Fzd10 but not Fzd9 to activate downstream β-catenin signaling in pulmonary fibrotic events [48].

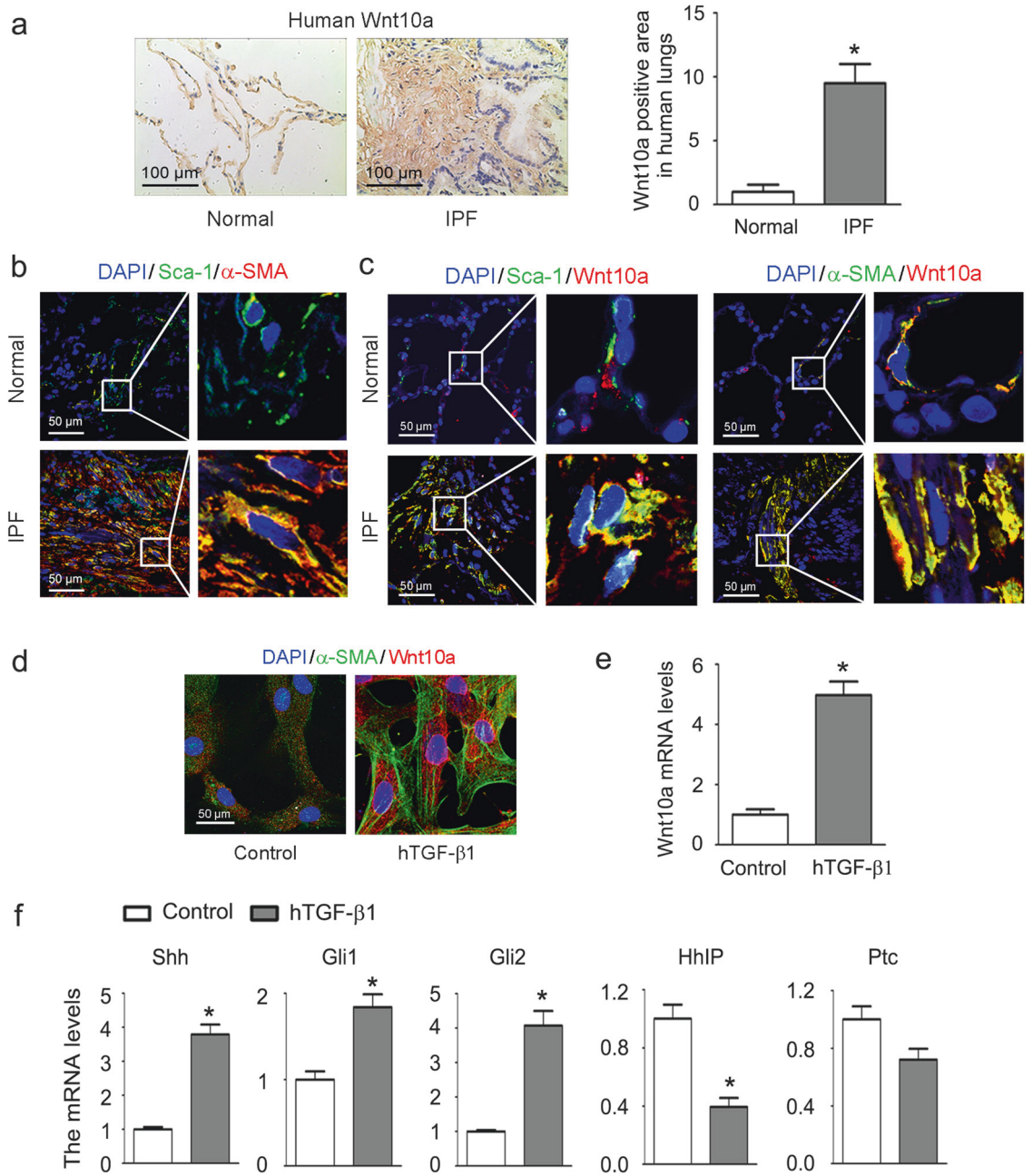

Fig. 6 Wnt10a overexpression and sonic hedgehog (Shh) pathway activation are found in human pulmonary fibrosis. **a** Wnt10a expression in lung sections from healthy subjects and patients with idiopathic pulmonary fibrosis (IPF) was analyzed using immunohistochemistry. The percentages of $Wnt10a^{+}$ areas in human lung tissues were quantified (*$P < 0.05$ versus normal). **b** The expression of α-smooth muscle actin (α-SMA) in stem cell antigen-1 $(Sca\text{-}1)^{+}$ human lung-resident mesenchymal stem cells (LR-MSCs) was assessed by immunofluorescence. **c** Colocalization of Wnt10a and Sca-1 or α-SMA in human lung tissues was examined by confocal fluorescence microscopy. Human LR-MSCs were treated with 10 ng/ml human transforming growth factor-β1 (hTGF-β1) for 48 h followed by the measurement of the expression of α-SMA and Wnt10a using immunofluorescence (**d**) and the measurement of the mRNA levels of Wnt10a (**e**) and hedgehog pathway components (**f**) using qRT-PCR. The results are shown as the means ± SD (*$P < 0.05$ versus control)

We further established the clinical relevance of our findings to the pathogenesis of human lung fibrosis. Since fresh IPF lung tissues were not readily available, we isolated human LR-MSCs from the lungs of patients undergoing pneumonectomy for pneumothorax. Our analyses of lung sections from IPF patients and of human LR-MSCs undergoing myofibroblastic differentiation suggested that Wnt10a overexpression was correlated with Shh/Gli signaling cascade activation. This discovery provides strong support for further research that might help clarify the

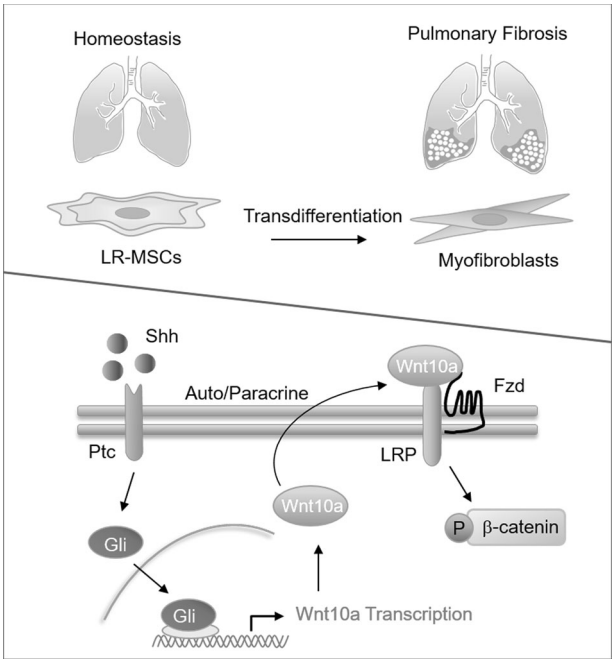

Fig. 7 Proposed model for hedgehog-Wnt signaling in the modulation of pulmonary fibrosis. During pulmonary fibrosis, sonic hedgehog (Shh) signaling is activated, and lung-resident mesenchymal stem cells (LR-MSCs) are the responsive cells. Shh interacts with the patched (Ptc) receptor to initiate a series of intracellular events that activate glioblastoma (Gli) factors, which subsequently translocate to the nucleus and promote the transcription of Wnt10a through binding with its promoter. Next, secreted Wnt10a acts on the surrounding LR-MSCs in an autocrine or paracrine manner. In the presence of Wnt10a, low-density lipoprotein receptor-related protein (LRP) forms a complex with Wnt-bound Frizzled (Fzd). Formation of this complex leads to nuclear translocation of active β-catenin, triggering myofibroblastic differentiation of LR-MSCs and pulmonary fibrosis. Accordingly, inhibition of the hedgehog-Wnt signaling can efficiently suppress the pulmonary fibrotic events

pathogenesis of pulmonary fibrosis and lead to novel therapies to improve recovery from IPF.

Acknowledgements This work was supported by the National Natural Science Foundation of China (81570059, 81172032) and the State Key Laboratory of Analytical Chemistry for Life Science (5431ZZXM1805).

Compliance with ethical standards

Conflict of interest The authors declare that they have no conflict of interest.

Ethical statement Animal experiments were conducted in accordance with the Guide for the Care and Use of Laboratory Animals (The Ministry of Science and Technology of China, 2006), and all experimental protocols were approved by the Animal Care and Use Committee of Nanjing University. Anonymized lung sections from five patients with IPF and five healthy control subjects were obtained from Nanjing Drum Tower Hospital. Lung samples from patients who provided written informed consent were used to prepare human LR-MSCs following permission from the ethics committee of Nanjing University. All methods were performed in accordance with the guidelines and regulations for human subject research.

References

1. Raghu G, Collard HR, Egan JJ, Martinez FJ, Behr J, Brown KK, et al. An official ATS/ERS/JRS/ALAT statement: idiopathic pulmonary fibrosis: evidence-based guidelines for diagnosis and management. Am J Respir Crit Care Med. 2011;183:788–824.
2. Raghu G, Weycker D, Edelsberg J, Bradford WZ, Oster G. Incidence and prevalence of idiopathic pulmonary fibrosis. Am J Respir Crit Care Med. 2006;174:810–6.
3. Gribbin J, Hubbard RB, Le Jeune I, Smith CJ, West J, Tata LJ. Incidence and mortality of idiopathic pulmonary fibrosis and sarcoidosis in the UK. Thorax. 2006;61:980–5.
4. Thannickal VJ, Toews GB, White ES, Lynch JP 3rd, Martinez FJ. Mechanisms of pulmonary fibrosis. Ann Rev Med. 2004;55:395–417.
5. Pittenger MF, Mackay AM, Beck SC, Jaiswal RK, Douglas R, Mosca JD, et al. Multilineage potential of adult human mesenchymal stem cells. Science. 1999;284:143–7.
6. da Silva Meirelles L, Chagastelles PC, Nardi NB. Mesenchymal stem cells reside in virtually all post-natal organs and tissues. J Cell Sci. 2006;119:2204–13.
7. Jun D, Garat C, West J, Thorn N, Chow K, Cleaver T, et al. The pathology of bleomycin-induced fibrosis is associated with loss of resident lung mesenchymal stem cells that regulate effector T-cell proliferation. Stem Cells. 2011;29:725–35.
8. Gong X, Sun Z, Cui D, Xu X, Zhu H, Wang L, et al. Isolation and characterization of lung resident mesenchymal stem cells capable of differentiating into alveolar epithelial type II cells. Cell Biol Int. 2014;38:405–11.
9. Hegab AE, Kubo H, Fujino N, Suzuki T, He M, Kato H, et al. Isolation and characterization of murine multipotent lung stem cells. Stem Cells Dev. 2010;19:523–36.
10. Salazar KD, Lankford SM, Brody AR. Mesenchymal stem cells produce Wnt isoforms and TGF-beta1 that mediate proliferation and procollagen expression by lung fibroblasts. Am J Physiol Lung Cell Mol Physiol. 2009;297:L1002–11.
11. Foronjy RF, Majka SM. The potential for resident lung mesenchymal stem cells to promote functional tissue regeneration: understanding microenvironmental cues. Cells. 2012;1:874.
12. Hou J, Ma T, Cao H, Chen Y, Wang C, Chen X, et al. TNF-alpha-induced NF-kappaB activation promotes myofibroblast differentiation of LR-MSCs and exacerbates bleomycin-induced pulmonary fibrosis. J Cell Physiol. 2018;233:2409–19.
13. Peng YY, He YH, Chen C, Xu T, Li L, Ni MM, et al. NLRC5 regulates cell proliferation, migration and invasion in hepatocellular carcinoma by targeting the Wnt/beta-catenin signaling pathway. Cancer Lett. 2016;376:10–21.
14. Nusse R, Clevers H. Wnt/beta-catenin signaling, disease, and emerging therapeutic modalities. Cell. 2017;169:985–99.
15. Taurin S, Sandbo N, Qin Y, Browning D, Dulin NO. Phosphorylation of beta-catenin by cyclic AMP-dependent protein kinase. J Biol Chem. 2006;281:9971–6.
16. Konigshoff M, Balsara N, Pfaff EM, Kramer M, Chrobak I, Seeger W, et al. Functional Wnt signaling is increased in idiopathic pulmonary fibrosis. PloS ONE. 2008;3:e2142.
17. Meuten T, Hickey A, Franklin K, Grossi B, Tobias J, Newman DR, et al. WNT7B in fibroblastic foci of idiopathic pulmonary fibrosis. Respir Res. 2012;13:62.

18. Katoh M, Katoh M. Transcriptional regulation of WNT2B based on the balance of Hedgehog, Notch, BMP and WNT signals. Int J Oncol. 2009;34:1411–5.
19. Yang SH, Andl T, Grachtchouk V, Wang A, Liu J, Syu LJ, et al. Pathological responses to oncogenic Hedgehog signaling in skin are dependent on canonical Wnt/beta3-catenin signaling. Nat Genet. 2008;40:1130–5.
20. Cigna N, Farrokhi Moshai E, Brayer S, Marchal-Somme J, Wemeau-Stervinou L, Fabre A, et al. The hedgehog system machinery controls transforming growth factor-beta-dependent myofibroblastic differentiation in humans: involvement in idiopathic pulmonary fibrosis. Am J Pathol. 2012;181:2126–37.
21. Bolanos AL, Milla CM, Lira JC, Ramirez R, Checa M, Barrera L, et al. Role of sonic hedgehog in idiopathic pulmonary fibrosis. Am J Physiol Lung Cell Mol Physiol. 2012;303:L978–90.
22. Kramann R, Schneider RK, DiRocco DP, Machado F, Fleig S, Bondzie PA, et al. Perivascular Gli1+ progenitors are key contributors to injury-induced organ fibrosis. Cell Stem Cell. 2015;16:51–66.
23. Omenetti A, Yang L, Li YX, McCall SJ, Jung Y, Sicklick JK, et al. Hedgehog-mediated mesenchymal-epithelial interactions modulate hepatic response to bile duct ligation. Lab Investig. 2007;87:499–514.
24. Fuccillo M, Joyner AL, Fishell G. Morphogen to mitogen: the multiple roles of hedgehog signalling in vertebrate neural development. Nat Rev Neurosci. 2006;7:772–83.
25. Kalderon D. Transducing the hedgehog signal. Cell. 2000;103: 371–4.
26. Chanda D, Otoupalova E, Smith SR, Volckaert T, De Langhe SP, Thannickal VJ. Developmental pathways in the pathogenesis of lung fibrosis. Mol Asp Med. 2018;65:56–69.
27. Chuang PT, Kawcak T, McMahon AP. Feedback control of mammalian Hedgehog signaling by the Hedgehog-binding protein, Hip1, modulates Fgf signaling during branching morphogenesis of the lung. Genes Dev. 2003;17:342–7.
28. Shi C, Lv T, Xiang Z, Sun Z, Qian W, Han X. Role of Wnt/beta-catenin signaling in epithelial differentiation of lung resident mesenchymal stem cells. J Cell Biochem. 2015; 116:1532–9.
29. Rolandsson S, Andersson Sjoland A, Brune JC, Li H, Kassem M, Mertens F, et al. Primary mesenchymal stem cells in human transplanted lungs are CD90/CD105 perivascularly located tissue-resident cells. BMJ Open Respir Res. 2014;1:e000027.
30. Lauth M, Bergstrom A, Shimokawa T, Toftgard R. Inhibition of GLI-mediated transcription and tumor cell growth by small-moleculeantagonists. Proc Natl Acad Sci USA. 2007;104: 8455–60.
31. Lu D, Choi MY, Yu J, Castro JE, Kipps TJ, Carson DA. Salinomycin inhibits Wnt signaling and selectively induces apoptosis in chronic lymphocytic leukemia cells. Proc Natl Acad Sci USA. 2011;108:13253–7.
32. Sun Z, Wang Y, Gong X, Su H, Han X. Secretion of rat tracheal epithelial cells induces mesenchymal stem cells to differentiate into epithelial cells. Cell Biol Int. 2012;36:169–75.
33. Chilosi M, Poletti V, Zamo A, Lestani M, Montagna L, Piccoli P, et al. Aberrant Wnt/beta-catenin pathway activation in idiopathic pulmonary fibrosis. Am J Pathol. 2003;162:1495–502.
34. Selman M, Pardo A, Barrera L, Estrada A, Watson SR, Wilson K, et al. Gene expression profiles distinguish idiopathic pulmonary fibrosis from hypersensitivity pneumonitis. Am J Respir Crit Care Med. 2006;173:188–98.
35. Katoh M. Networking of WNT, FGF, Notch, BMP, and Hedgehog signaling pathways during carcinogenesis. Stem Cell Rev. 2007;3:30–8.
36. Kramann R, Schneider RK. The identification of fibrosis-driving myofibroblast precursors reveals new therapeutic avenues in myelofibrosis. Blood. 2018;131:2111–9.
37. Fernandez IE, Eickelberg O. New cellular and molecular mechanisms of lung injury and fibrosis in idiopathic pulmonary fibrosis. Lancet. 2012;380:680–8.
38. Henderson WR Jr., Chi EY, Ye X, Nguyen C, Tien YT, et al. Inhibition of Wnt/beta-catenin/CREB binding protein (CBP) signaling reverses pulmonary fibrosis. Proc Natl Acad Sci USA. 2010;107:14309–14.
39. He W, Dai C, Li Y, Zeng G, Monga SP, Liu Y. Wnt/beta-catenin signaling promotes renal interstitial fibrosis. J Am Soc Nephrol. 2009;20:765–76.
40. Bayle J, Fitch J, Jacobsen K, Kumar R, Lafyatis R, Lemaire R. Increased expression of Wnt2 and SFRP4 in Tsk mouse skin: role of Wnt signaling in altered dermal fibrillin deposition and systemic sclerosis. J Investig Dermatol. 2008;128:871–81.
41. Shu DY, Lovicu FJ. Myofibroblast transdifferentiation: the dark force in ocular wound healing and fibrosis. Prog Retin Eye Res. 2017;60:44–65.
42. Etheridge SL, Spencer GJ, Heath DJ, Genever PG. Expression profiling and functional analysis of wnt signaling mechanisms in mesenchymal stem cells. Stem cells. 2004;22:849–60.
43. Rankin SA, Han L, McCracken KW, Kenny AP, Anglin CT, Grigg EA, et al. A retinoic acid-hedgehog cascade coordinates mesoderm-inducing signals and endoderm competence during lung specification. Cell Rep. 2016;16:66–78.
44. He H, Du F, He Y, Wei Z, Meng C, Xu Y, et al. The Wnt-beta-catenin signaling regulated MRTF-A transcription to activate migration-related genes in human breast cancer cells. Oncotarget. 2018;9:15239–51.
45. Zheng G, Tao Y, Yu W, Schwartz RJ. Brief report: SRF-dependent MiR-210 silences the sonic hedgehog signaling during cardiopoesis. Stem Cells. 2013;31:2279–85.
46. Oda K, Yatera K, Izumi H, Ishimoto H, Yamada S, Nakao H, et al. Profibrotic role of WNT10A via TGF-beta signaling in idiopathic pulmonary fibrosis. Respir Res. 2016;17:39.
47. Yu F, Fan X, Chen B, Dong P, Zheng J. Activation of hepatic stellate cells is inhibited by microRNA-378a-3p via Wnt10a. Cell Physiol Biochem. 2016;39:2409–20.
48. Chen X, Shi C, Cao H, Chen L, Hou J, Xiang Z, et al. The hedgehog and Wnt/beta-catenin system machinery mediate myofibroblast differentiation of LR-MSCs in pulmonary fibrogenesis. Cell Death Dis. 2018;9:639.